2011 50th IEEE Conference on Decision and Control and
European Control Conference (CDC-ECC)
Orlando, FL, USA, December 12-15, 2011

Portraits of cyclic pursuit

K. S. Galloway, E. W. Justh, and P. S. Krishnaprasad

Abstract— **The study of cyclic pursuit as a means to collective behavior in nature and in artificial multi-agent systems is of current interest. Here we examine the nonlinear closed loop dynamics of planar cyclic pursuit based on the constant bearing (CB) strategy. We show that there exists a family of rectilinear relative equilibria that admit nearby periodic orbits in an appropriate low dimensional space found by methods of symmetry, reduction and constraint. We also demonstrate the existence of other families of rectilinear equilibria that exhibit attractivity or instability.**

I. Introduction

Prior work on planar cyclic pursuit as a building block for collective behavior has yielded insights on relative equilibria, and invariant manifolds with applications (see, for instance, [1], [2], [3], [4], [5], and [6]). The present work focuses on closed loop nonlinear dynamics. A surprising result is the presence of previously unknown periodic orbits associated to the CB strategy in the 3-agent planar problem. While some of the techniques we employ in symmetry and reduction have parallels in recent work on periodic orbits in the Newtonian 3-body problem [7], the present context of gyroscopic interaction is very different from the setting of celestial mechanics.

As exemplified by figure 2, the current work proceeds as follows. In section II we describe the mathematical framework for modeling the state (i.e. positions and orientations with respect to a fixed coordinate frame) of a system of n agents moving at unit speed, defining our $3n$-dimensional state space M_{state} in (2). We then illustrate a reduction to the $(3n-3)$-dimensional quotient manifold $M_{state}/SE(2)$ and prescribe an alternative parametrization to that described in [1]. (See **Proposition 1**.) It should be noted that the results of section II are applicable for any set of $SE(2)$-invariant control laws u_i. In section III we define a $(2n-3)$-dimensional submanifold $M_{CB(\boldsymbol{\alpha})} \subset M_{state}/SE(2)$ which is associated with the *constant bearing (CB)* pursuit strategy in a *cyclic pursuit* framework (i.e. agent i pursues agent $i+1$ modulo n). In **Proposition 2**, it is demonstrated that the CB pursuit law defined in [8] (as described in (11)) yields closed-loop cyclic CB pursuit dynamics under which $M_{CB(\boldsymbol{\alpha})}$ is invariant and attractive. Reduced dynamics on $M_{CB(\boldsymbol{\alpha})}$ are stated in (16), which are subject to the "closure" constraints (17) and (18).

In section IV, we demonstrate how a scaling of the time variable enables a further reduction to the $(2n-4)$-dimensional submanifold $\bar{M}_{CB(\boldsymbol{\alpha})} \subset M_{CB(\boldsymbol{\alpha})}$. Although the reduction step is valid for arbitrary values of n, we describe the process in the particular context of the $n=3$ case, yielding a two-dimensional reduced dynamics on $\bar{M}_{CB(\boldsymbol{\alpha})}$ in (30)-(31). In terms of these reduced dynamics we are able to analyze stability properties of a particular type of rectilinear equilibrium for the three-particle case, as discussed in section V. For a particular choice of parameters, phase portrait analysis reveals the existence of periodic orbits in the two-dimensional system leading to remarkable precessing motions of the three-body system in the full physical space. (See figure 7.) We conclude in section VI with a mention of work in progress.

II. Modeling

As described in [1], we model our system of n agents as unit-mass particles tracing out twice-differentiable curves in the plane. The state of the i^{th} particle (i.e. agent) with respect to a fixed inertial frame can be described by a position vector $\mathbf{r}_i$ and the respective natural Frenet frame $\{\mathbf{x}_i, \mathbf{y}_i\}$, where $\mathbf{x}_i$ is the unit vector tangent to the curve at that point and $\mathbf{y}_i$ is the unit normal [1]. If we constrain each agent to move at (constant) unit speed, then our system dynamics are given by

$$\begin{aligned} \dot{\mathbf{r}}_i &= \mathbf{x}_i, \\ \dot{\mathbf{x}}_i &= \mathbf{y}_i u_i, \\ \dot{\mathbf{y}}_i &= -\mathbf{x}_i u_i, \ i = 1, 2, \ldots, n, \end{aligned} \tag{1}$$

where u_i is the signed curvature, viewed as a steering control. Note that u_i can be specified as a feedback law in terms of the state variables. Defining the baseline vector $\mathbf{r}_{i,i+1} = \mathbf{r}_i - \mathbf{r}_{i+1}$ and imposing an additional constraint prohibiting "sequential colocation" (i.e. we assume $|\mathbf{r}_{i,i+1}| > 0$ for all t), our state space can then be described as

$$\begin{aligned} M_{state} = \Big\{ &(\mathbf{r}_1, \mathbf{x}_1, \mathbf{y}_1, \ldots, \mathbf{r}_n, \mathbf{x}_n, \mathbf{y}_n) \mid \\ &\mathbf{r}_{i,i+1} \neq \mathbf{0}, \ i = 1, 2, \ldots, n \Big\}, \end{aligned} \tag{2}$$

where it is understood that $\mathbf{r}_i \in \mathbb{R}^2$ and the pair of unit vectors $\{\mathbf{x}_i, \mathbf{y}_i\}$ comprise an orthonormal frame.

We note that each pair of frame vectors can be parametrized by a single angle variable (i.e. $[\mathbf{x}_i, \mathbf{y}_i] \in SO(2) \cong S^1$) and therefore M_{state} is $3n$-dimensional.

This research was supported in part by the Air Force Office of Scientific Research under AFOSR grant FA95501010250; by an L-3 Communications Graduate Fellowship; by the ODDR&E MURI2007 Program Grant N000140710734 (through the Office of Naval Research); and by the Office of Naval Research.

K.S. Galloway and P.S. Krishnaprasad are with the Institute for Systems Research and the Department of Electrical and Computer Engineering at the University of Maryland, College Park, MD 20742, USA. kgallow1@umd.edu, krishna@umd.edu

E.W. Justh is with the Naval Research Laboratory, Washington, DC 20375, USA.

We are interested in steering laws u_i which leave our system dynamics (1) invariant under the action of the special Euclidean group SE(2). (A particular pursuit law of this form will be discussed in section III.) As in [1], steering laws of this type (and the resultant closed-loop dynamics) permit a reduction to the $(3n-3)$-dimensional quotient manifold $M_{state}/SE(2)$, the **shape space**, which describes the relative positions and velocities of the agents. The following proposition prescribes a system of shape variables[1] for parametrization of $M_{state}/SE(2)$.

Proposition 1: Let $R(\cdot) \in SO(2)$ be the rotation matrix defined by

$$R(\beta) = \begin{bmatrix} \cos(\beta) & -\sin(\beta) \\ \sin(\beta) & \cos(\beta) \end{bmatrix}, \tag{3}$$

and define $\kappa_i, \theta_i \in [0, 2\pi)$ and $\rho_i \in \mathbb{R}^+$ by

$$R(\kappa_i)\mathbf{x}_i \cdot \frac{\mathbf{r}_{i,i+1}}{|\mathbf{r}_{i,i+1}|} = -1, \quad R(\theta_i)\mathbf{x}_i \cdot \frac{\mathbf{r}_{i-1,i}}{|\mathbf{r}_{i-1,i}|} = 1,$$
$$\rho_i = |\mathbf{r}_{i,i+1}|, \ i = 1, 2, \ldots, n. \tag{4}$$

(See figure 1.) Then the shape space $M_{state}/SE(2)$ can be parametrized by $\{(\kappa_i, \theta_i, \rho_i),\ i = 1, 2, \ldots, n\}$, subject to $\rho_i > 0,\ i = 1, 2, \ldots, n$ and the constraint equations

$$R\left(\sum_{i=1}^{n}(\pi + \kappa_i - \theta_i)\right) = \mathbb{1}, \text{ the } 2 \times 2 \text{ identity matrix}, \tag{5}$$

$$\sum_{i=1}^{n} \rho_i R\left(\sum_{j=1}^{i}(\pi + \kappa_j - \theta_j)\right) = 0. \tag{6}$$

Proof: Omitted due to space constraints.

Remark: The stipulation that $\rho_i > 0$ follows from our prohibition on sequential colocation in the definition of M_{state}. The "closure" constraints (5) and (6) constrain three degrees of freedom and result from the fact that we have parametrized a $(3n-3)$-dimensional space with $3n$ variables. One can show that (5) and (6) are preserved under the shape dynamics (as stated below) and can therefore be viewed as a constraint on the initial conditions.

It is a relatively straightforward exercise to demonstrate that in terms of the shape variables from **Proposition 1**, our dynamics on $M_{state}/SE(2)$ are given by

$$\begin{aligned} \dot{\kappa}_i &= -u_i + \frac{1}{\rho_i}\left[\sin(\kappa_i) + \sin(\theta_{i+1})\right], \\ \dot{\theta}_i &= -u_i + \frac{1}{\rho_{i-1}}\left[\sin(\kappa_{i-1}) + \sin(\theta_i)\right], \\ \dot{\rho}_i &= -\cos(\kappa_i) - \cos(\theta_{i+1}), \end{aligned} \tag{7}$$

with initial conditions subject to the constraints (5) and (6).

[1]Note that the shape variables here give a parametrization equivalent to that developed in [1].

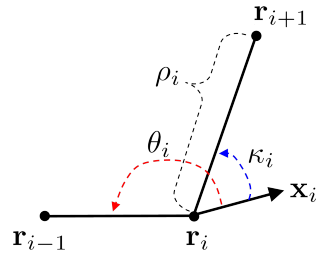

Fig. 1. Illustration of the shape variables used to parametrize the shape space $M_{state}/SE(2)$.

III. Constant Bearing Pursuit

The current work is focused on the particular context of n-agent *cyclic pursuit* systems (i.e. agent i pursues agent $i+1$ modulo n) in which each agent employs a *constant bearing (CB)* pursuit strategy. The CB pursuit strategy extends the concept of classical pursuit (i.e. "always move directly towards the current location of the target") by prescribing a fixed, possibly non-zero angle α_i between the pursuer's heading and the current location of the target. Note that for purposes of our analysis in this work, we do not constrain α_i to be acute but permit it to take the full range of values $\alpha_i \in [0, 2\pi)$.

In terms of our original state variables, if we define the cost function

$$\Lambda_i \triangleq R(\alpha_i)\mathbf{x}_i \cdot \frac{\mathbf{r}_{i,i+1}}{|\mathbf{r}_{i,i+1}|}, \tag{8}$$

then we say agent i has attained CB pursuit of agent $i+1$ if and only if $\Lambda_i = -1$. In terms of our shape variables, the cost function Λ_i is given by

$$\Lambda_i = -\cos(\kappa_i - \alpha_i). \tag{9}$$

For an n-agent cyclic pursuit system in which each agent i employs the CB pursuit strategy with regard to agent $i+1$ (modulo n), we define the $(2n-3)$-dimensional CB Pursuit Manifold $M_{CB(\boldsymbol{\alpha})} \subset M_{state}/SE(2)$ by

$$M_{CB(\boldsymbol{\alpha})} = \Big\{(\kappa_1, \theta_1, \rho_1, \ldots, \kappa_n, \theta_n, \rho_n) \in M_{state}/SE(2) \mid \Lambda_i = -1, i = 1, 2, \ldots, n\Big\}, \tag{10}$$

where $\boldsymbol{\alpha} = (\alpha_1, \alpha_2, \ldots, \alpha_n)$.

A feedback law designed to attain the CB pursuit strategy was developed in [8], and it takes the form

$$u_{CB(\alpha_i)} = -\mu_i \left(R(\alpha_i)\mathbf{y}_i \cdot \frac{\mathbf{r}_{i,i+1}}{|\mathbf{r}_{i,i+1}|}\right) - \frac{1}{|\mathbf{r}_{i,i+1}|}\left(\frac{\mathbf{r}_{i,i+1}}{|\mathbf{r}_{i,i+1}|} \cdot \dot{\mathbf{r}}^{\perp}_{i,i+1}\right), \tag{11}$$

where $\mu_i > 0$ is a control gain, and $\mathbf{b}^{\perp}$ denotes $R\left(\frac{\pi}{2}\right)\mathbf{b}$. In terms of our shape variables, the pursuit law $u_{CB(\alpha_i)}$ is given by

$$u_{CB(\alpha_i)} = \mu_i \sin(\kappa_i - \alpha_i) + \frac{1}{\rho_i}\left[\sin(\kappa_i) + \sin(\theta_{i+1})\right]. \tag{12}$$

If every agent uses a pursuit law of this form, then by substitution into (7) we have the closed-loop cyclic CB pursuit dynamics

$$\begin{aligned}
\dot{\kappa}_i &= -\mu_i \sin(\kappa_i - \alpha_i), \\
\dot{\theta}_i &= -\mu_i \sin(\kappa_i - \alpha_i) + \frac{1}{\rho_{i-1}} \left[\sin(\kappa_{i-1}) + \sin(\theta_i)\right] \\
&\quad - \frac{1}{\rho_i} \left[\sin(\kappa_i) + \sin(\theta_{i+1})\right], \\
\dot{\rho}_i &= -\cos(\kappa_i) - \cos(\theta_{i+1}),\ i = 1, 2, \ldots, n,
\end{aligned} \tag{13}$$

with initial conditions subject to the constraint equations given by (5) and (6). The following proposition describes certain properties of the submanifold $M_{CB(\boldsymbol{\alpha})}$ under the shape dynamics (13).

Proposition 2: The submanifold $M_{CB(\boldsymbol{\alpha})} \subset M_{state}/SE(2)$ is invariant under the dynamics (13), and any bounded trajectory of (13) starting in the set

$$\begin{aligned}
\Omega_\epsilon = \Big\{ &(\kappa_1, \theta_1, \rho_1, \ldots, \kappa_n, \theta_n, \rho_n) \in M_{state}/SE(2) \ \Big| \\
&\Lambda_i \leq 1 - \epsilon,\ i = 1, 2, \ldots, n \Big\}
\end{aligned} \tag{14}$$

(for $0 < \epsilon \leq 2$) converges asymptotically to $M_{CB(\boldsymbol{\alpha})}$.

Proof: By inspection of (9), we note that $\Lambda_i = -1 \iff \kappa_i = \alpha_i$. From (13) we have $\kappa_i = \alpha_i \implies \dot{\kappa}_i = 0$, and therefore we conclude that $M_{CB(\boldsymbol{\alpha})}$ is invariant under (13). Note that Ω_ϵ is closed (but not necessarily bounded) and excludes states for which $\Lambda_i = +1$ for any i. Then defining $\Lambda = \sum_{i=1}^n \Lambda_i$ in terms of (9), we have

$$\dot{\Lambda} = \sum_{i=1}^n \dot{\kappa}_i \sin(\kappa_i - \alpha_i) = \sum_{i=1}^n -\mu_i \left(1 - \Lambda_i^2\right), \tag{15}$$

and therefore $\dot{\Lambda} \leq 0$ on Ω_ϵ with $\dot{\Lambda} = 0$ on Ω_ϵ if and only if $\Lambda_i = -1,\ i = 1, 2, \ldots, n$. The hypothesis of boundedness of the trajectory ensures by Birkhoff's theorem the ω-limit set is nonempty, compact and invariant. Asymptotic convergence to $M_{CB(\boldsymbol{\alpha})}$ follows as in the steps in the proof of LaSalle's Invariance Principle [9]. □

We can formulate reduced dynamics on $M_{CB(\boldsymbol{\alpha})}$ by substituting $\kappa_i \equiv \alpha_i$ into (13) to arrive at

$$\begin{aligned}
\dot{\theta}_i &= \frac{1}{\rho_{i-1}} \left[\sin(\alpha_{i-1}) + \sin(\theta_i)\right] - \frac{1}{\rho_i} \left[\sin(\alpha_i) + \sin(\theta_{i+1})\right], \\
\dot{\rho}_i &= -\left[\cos(\alpha_i) + \cos(\theta_{i+1})\right],\ i = 1, 2, \ldots, n,
\end{aligned} \tag{16}$$

with the initial conditions subject to the constraints

$$R\left(\sum_{i=1}^n (\pi + \alpha_i - \theta_i)\right) = \mathbb{1}, \tag{17}$$

$$\sum_{i=1}^n \rho_i R\left(\sum_{j=1}^i (\pi + \alpha_j - \theta_j)\right) = 0. \tag{18}$$

Remark: The definition of $M_{CB(\boldsymbol{\alpha})}$ and proof of invariance under the dynamics given by (13) is analogous to that presented in [1].

IV. Reduction to pure shape dynamics on $M_{CB(\boldsymbol{\alpha})}$

In this section we illustrate a process for further reduction to a $(2n-4)$-dimensional submanifold. Although this process is applicable for arbitrary values of n, in the interest of concreteness we will present the reduction process in the context of the three-particle case. For $n = 3$, $M_{CB(\boldsymbol{\alpha})}$ is a three-dimensional submanifold parametrized by the shape variables $\theta_1, \theta_2, \theta_3, \rho_1, \rho_2, \rho_3$, subject to the constraint equations (17) and (18). As a first step, we eliminate θ_1, θ_3, and ρ_3 by means of (17) and (18) so that we can explicitly describe our shape dynamics in terms of only θ_2, ρ_1, and ρ_2. We do so by first noting that (17) implies

$$\sum_{i=1}^3 (\pi + \alpha_i - \theta_i) = 0, \tag{19}$$

and therefore $\theta_1 = \pi + \alpha_1 + \alpha_2 + \alpha_3 - \theta_2 - \theta_3$. Then substitution into (18) yields

$$\begin{aligned}
0 &= \rho_1 R(\pi + \alpha_1 - \theta_1) + \rho_2 R(\alpha_1 + \alpha_2 - \theta_1 - \theta_2) + \rho_3 \mathbb{1} \\
&= \rho_1 R(-\alpha_2 - \alpha_3 + \theta_2 + \theta_3) + \rho_2 R(\pi - \alpha_3 + \theta_3) + \rho_3 \mathbb{1} \\
&= R(\theta_3) \Big[\rho_1 R(\theta_2 - \alpha_2 - \alpha_3) \\
&\qquad + \rho_2 R(\pi - \alpha_3) + \rho_3 R(-\theta_3) \Big],
\end{aligned} \tag{20}$$

and since elements of $SO(2)$ are nonsingular (i.e. $R(\theta_3)$ is nonsingular), we have

$$\begin{aligned}
\rho_3 \sin(\theta_3) &= \rho_1 \sin(\theta_2 - \alpha_2 - \alpha_3) + \rho_2 \sin(\alpha_3), \\
\rho_3 \cos(\theta_3) &= -\rho_1 \cos(\theta_2 - \alpha_2 - \alpha_3) + \rho_2 \cos(\alpha_3).
\end{aligned} \tag{21}$$

By summing the square of each equation in (21), we have

$$\begin{aligned}
\rho_3^2 &= \rho_1^2 - 2\rho_1\rho_2 \cos(\theta_2 - \alpha_2) + \rho_2^2 \\
&= \rho_1^2 \left[1 - 2\left(\frac{\rho_2}{\rho_1}\right) \cos(\theta_2 - \alpha_2) + \left(\frac{\rho_2}{\rho_1}\right)^2\right],
\end{aligned} \tag{22}$$

which, by the strict positivity of ρ_3, yields

$$\rho_3 = \rho_1 P(\rho_1, \rho_2, \theta_2), \tag{23}$$

where $P(\rho_1, \rho_2, \theta_2) \triangleq \sqrt{\left(\frac{\rho_2}{\rho_1}\right)^2 - 2\left(\frac{\rho_2}{\rho_1}\right) \cos(\theta_2 - \alpha_2) + 1}$. We restrict our analysis to M_{state} (i.e. no sequential colocation), and thus we forbid $\rho_1 = \rho_2$ with $\theta_2 = \alpha_2$ which is the only condition under which $P(\rho_1, \rho_2, \theta_2) = 0$. Then substituting (21) and (23) into (16), we have an equivalent representation of our three-particle shape dynamics on $M_{CB(\boldsymbol{\alpha})}$, given by

$$\begin{aligned}
\dot{\theta}_2 &= \frac{1}{\rho_1} \left[\sin(\alpha_1) + \sin(\theta_2)\right] \\
&\quad - \frac{1}{\rho_2} \left[\sin(\alpha_2) + \frac{\sin(\theta_2 - \alpha_2 - \alpha_3) + \frac{\rho_2}{\rho_1} \sin(\alpha_3)}{P(\rho_1, \rho_2, \theta_2)}\right], \\
\dot{\rho}_1 &= -\cos(\alpha_1) - \cos(\theta_2), \\
\dot{\rho}_2 &= -\cos(\alpha_2) - \frac{-\cos(\theta_2 - \alpha_2 - \alpha_3) + \frac{\rho_2}{\rho_1} \cos(\alpha_3)}{P(\rho_1, \rho_2, \theta_2)}.
\end{aligned} \tag{24}$$

These dynamics are subject only to the strict positivity constraints on ρ_1, ρ_2, and $P(\rho_1, \rho_2, \theta_2)$.

Letting

$$\lambda \triangleq \ln(\rho_2/\rho_1) \tag{25}$$

and denoting

$$P \triangleq \sqrt{e^{2\lambda} - 2e^{\lambda}\cos(\theta_2 - \alpha_2) + 1}, \tag{26}$$

we have

$$\begin{aligned}
\dot{\lambda} &= \frac{1}{e^{\lambda}\rho_1 P}\Bigg\{P\left[e^{\lambda}\Big(\cos(\alpha_1) + \cos(\theta_2)\Big) - \cos(\alpha_2)\right] \\
&\quad + \cos(\theta_2 - \alpha_2 - \alpha_3) - e^{\lambda}\cos(\alpha_3)\Bigg\}, \\
\dot{\theta}_2 &= \frac{1}{e^{\lambda}\rho_1 P}\Bigg\{P\left[e^{\lambda}\Big(\sin(\alpha_1) + \sin(\theta_2)\Big) - \sin(\alpha_2)\right] \\
&\quad - \sin(\theta_2 - \alpha_2 - \alpha_3) - e^{\lambda}\sin(\alpha_3)\Bigg\},
\end{aligned} \tag{27}$$

with $\dot{\rho}_1$ defined as in (24). We then introduce a scaling of the time variable

$$\tau \triangleq \int_0^t \frac{1}{e^{\lambda(\sigma)}\rho_1(\sigma)P(\sigma)}d\sigma, \tag{28}$$

so that

$$\frac{d\theta_2}{d\tau} = \frac{d\theta_2}{dt}\frac{dt}{d\tau} = \dot{\theta}_2 e^{\lambda(t)}\rho_1(t)P(t). \tag{29}$$

(Note that an analogous statement holds for $\frac{d\lambda}{d\tau}$ and $\frac{d\rho_1}{d\tau}$.) Letting the prime superscript denote differentiation with respect to the scaled time variable τ, we then have

$$\begin{aligned}
\theta_2' &= P\left[e^{\lambda}\Big(\sin(\alpha_1) + \sin(\theta_2)\Big) - \sin(\alpha_2)\right] \\
&\quad - \sin(\theta_2 - \alpha_2 - \alpha_3) - e^{\lambda}\sin(\alpha_3), \qquad (30) \\
\lambda' &= P\left[e^{\lambda}\Big(\cos(\alpha_1) + \cos(\theta_2)\Big) - \cos(\alpha_2)\right] \\
&\quad + \cos(\theta_2 - \alpha_2 - \alpha_3) - e^{\lambda}\cos(\alpha_3), \qquad (31) \\
\rho_1' &= -e^{\lambda}\rho_1 P\left[\cos(\alpha_1) + \cos(\theta_2)\right]. \qquad (32)
\end{aligned}$$

As a result of the new time scale, (30) and (31) are a self-contained system in $\{\theta_2, \lambda\}$, permitting further reduction to the punctured cylinder

$$\bar{M}_{CB(\alpha_1,\alpha_2,\alpha_3)} = S^1 \times \mathbb{R} - \{(\alpha_2, 0)\}. \tag{33}$$

(As discussed previously, the deletion of the point $\{(\alpha_2, 0)\}$ is necessary to maintain our prohibition on sequential colocation, but it is not enforced by the dynamics (30) and (31).) Note that $\{\theta_2, \lambda\}$ describe the **pure shape** of the system, i.e. a triangle up to similarity.

Figure 2 provides a summary of the reduction process that we have described in the last two sections. While we have demonstrated the specific steps in the context of the three-particle case, it should be noted that the same process is applicable for the n-particle case and results in a reduction from a $3n$-dimensional system to a $(2n-4)$-dimensional system. In the current context (i.e. $n = 3$), this final reduction to a two-dimensional system greatly facilitates an analysis of system stability properties, since it permits techniques of phase plane analysis. In what follows, we use the two-dimensional dynamics (30)-(31) to analyze the stability properties of a particular family of rectilinear equilibria.

V. Stability analysis for a particular family of rectilinear equilibria

As discussed in [1], equilibria of the shape dynamics (13) correspond to relative equilibria of the full system dynamics (1). System dynamics of the form (1) permit *rectilinear* relative equilibria (i.e. all agents move along parallel rectilinear trajectories) as well as *circling* relative equilibria (i.e. all agents travel along a common closed circular trajectory of fixed radius, separated by fixed chordal distances). If we consider only the reduced system dynamics on $M_{CB(\boldsymbol{\alpha})}$, given by (16), then the discussion in [1] presents necessary and sufficient conditions for existence of each type of relative equilibria. Here we restate (without proof) the proposition concerning existence of rectilinear equilibria:

Proposition 3 (from [1]): Given $\{\alpha_1, \alpha_2, \ldots, \alpha_n\}$, a relative equilibrium corresponding to rectilinear motion on $M_{CB(\boldsymbol{\alpha})}$ exists for system (1) under cyclic pursuit with CB control law (11) if and only if there exists a set of constants $\{\sigma_1, \sigma_2, \ldots, \sigma_n\}$ such that $\sigma_i > 0,\ i = 1, 2, \ldots, n$ and

$$\sum_{i=1}^{n} \sigma_i e^{j\alpha_i} = 0, \tag{34}$$

where $j = \sqrt{-1}$.

For such a relative equilibrium, one can show from (16) that the corresponding equilibrium angles $\hat{\theta}_i$ and equilibrium side lengths $\hat{\rho}_i$ are given by

$$\hat{\theta}_i = \pi + \alpha_{i-1},\ \hat{\rho}_i = \sigma_i,\ i = 1, 2, \ldots, n. \tag{35}$$

We now consider the special case for which $\alpha_1 = \alpha_2 = \cdots = \alpha_{n-1} = \alpha = \pi + \alpha_n$, for some $\alpha \in [0, 2\pi)$. In this case, (34) is satisfied by setting $\sigma_i = \hat{\rho}_i$ where $\hat{\rho}_i$ are side lengths and $\hat{\rho}_n = \sum_{i=1}^{n-1}\hat{\rho}_i$, and therefore a rectilinear equilibrium exists. (A depiction of this type of rectilinear equilibrium is displayed in figure 3.)

Once again focusing on the three-particle case, we investigate stability properties of rectilinear equilibria on $M_{CB(\alpha,\alpha,\pi+\alpha)}$ by considering their projections onto the submanifold $\bar{M}_{CB(\alpha,\alpha,\pi+\alpha)}$ defined in (33). We start by substituting $\alpha_1 = \alpha_2 = \alpha = \pi + \alpha_3$ into (30)-(31) to arrive at

$$\begin{aligned}
\theta_2' &= P\left[e^{\lambda}\Big(\sin(\alpha) + \sin(\theta_2)\Big) - \sin(\alpha)\right] \\
&\quad - \sin(\theta_2 - 2\alpha + \pi) + e^{\lambda}\sin(\alpha), \\
\lambda' &= P\left[e^{\lambda}\Big(\cos(\alpha) + \cos(\theta_2)\Big) - \cos(\alpha)\right] \\
&\quad + \cos(\theta_2 - 2\alpha + \pi) + e^{\lambda}\cos(\alpha),
\end{aligned} \tag{36}$$

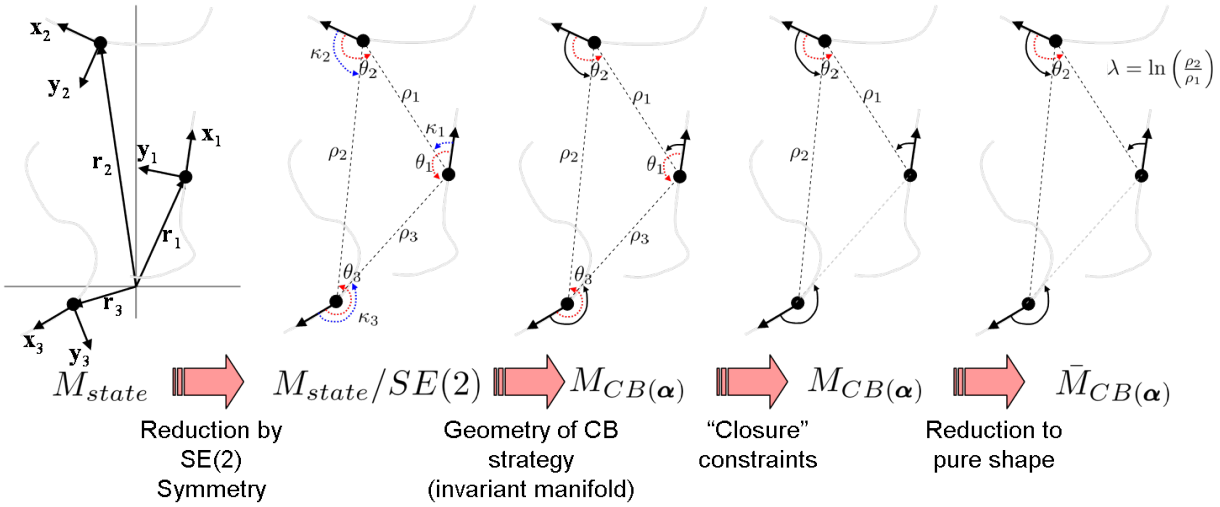

Fig. 2. This figure illustrates the process by which we reduce a $3n$-dimensional system to a $(2n-4)$-dimensional system by means of symmetry, geometry, and algebraic constraints. In each figure, the labeled variables are the quantities which are free to vary. Note that in the step from $M_{state}/SE(2)$ to $M_{CB(\boldsymbol{\alpha})}$ the dotted κ_i angles are replaced by solid black curves, indicating that $\kappa_i \equiv \alpha_i$ on $M_{CB(\boldsymbol{\alpha})}$ while θ_i angles remain free to vary.

where $P = \sqrt{e^{2\lambda} - 2e^{\lambda}\cos(\theta_2 - \alpha) + 1}$. We then define an angular error variable

$$\phi \triangleq \theta_2 - \hat{\theta}_2 = \theta_2 - \pi - \alpha, \tag{37}$$

so that $\phi = 0 \iff \theta_2 = \hat{\theta}_2$. Denoting

$$P \triangleq \sqrt{e^{2\lambda} + 2e^{\lambda}\cos(\phi) + 1}, \tag{38}$$

we can formulate $\{\phi, \lambda\}$ dynamics as

$$\begin{aligned} \phi^{'} &= P\left[e^{\lambda}\Big(\sin(\alpha) - \sin(\phi+\alpha)\Big) - \sin(\alpha)\right] \\ &\quad - \sin(\phi - \alpha) + e^{\lambda}\sin(\alpha), \\ \lambda^{'} &= P\left[e^{\lambda}\Big(\cos(\alpha) - \cos(\phi+\alpha)\Big) - \cos(\alpha)\right] \\ &\quad + \cos(\phi - \alpha) + e^{\lambda}\cos(\alpha). \end{aligned} \tag{39}$$

These dynamics evolve on a manifold (punctured cylinder) which is diffeomorphic to $\bar{M}_{CB(\alpha,\alpha,\pi+\alpha)}$ as defined in (33), and therefore we will consider the $\{\phi, \lambda\}$ dynamics as evolving on $\bar{M}_{CB(\alpha,\alpha,\pi+\alpha)}$. (The excluded point in terms of the $\{\phi, \lambda\}$ variables is given by $\phi = \pi, \lambda = 0$.) Then the set

$$\bar{M}_{\alpha} = \Big\{(\phi, \lambda) \in \bar{M}_{CB(\alpha,\alpha,\pi+\alpha)} \;\Big|\; \phi = 0\Big\} \tag{40}$$

denotes a continuum of equilibria for the dynamics given by (39), corresponding to a continuum of rectilinear equilibria for the full system. One can show that in fact $\bar{M}_{\alpha}$ contains *all* the equilibria for the dynamics (39). This can be demonstrated by first verifying that $\sin(\alpha)\lambda^{'} - \cos(\alpha)\phi^{'} = \sin(\phi)\big(1 + Pe^{\lambda}\big)$, from which it follows that $\phi^{'} = 0 = \lambda^{'} \implies \sin(\phi) = 0$. The claim then follows by verifying that $\phi = \pi$ can not correspond to an equilibrium for the dynamics.

Before proceeding with our stability analysis, we state the following proposition regarding a particular property of the vector field (39) in the vicinity of the set $\bar{M}_{\alpha}$.

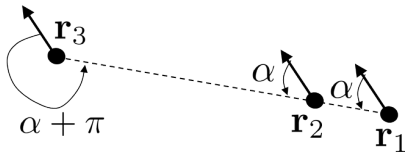

Fig. 3. Depiction of the type of rectilinear equilibrium which exists for the case where $\alpha_1 = \alpha_2 = \cdots = \alpha_{n-1} = \alpha = \pi + \alpha_n$, for some $\alpha \in [0, 2\pi)$.

Proposition 4: Let $\phi \in (0, \pi) \cup (\pi, 2\pi)$ so that

$$F(\phi, \lambda) \triangleq \frac{\partial \phi}{\partial \lambda}(\phi, \lambda) \tag{41}$$

is well-defined. Then for any fixed $\lambda_0 \in \mathbb{R}$,

$$\lim_{\phi \to 0} F(\phi, \lambda_0) = -\frac{\cos(\alpha)}{\sin(\alpha)}. \tag{42}$$

Proof: Omitted due to space constraints. Observe that $F(\phi, \lambda) = \phi^{'}/\lambda^{'}$, with $\phi^{'}$ and $\lambda^{'}$ as defined by (39). The proof then follows by applying L'Hôpital's rule to the limit calculation in (42).

We proceed with our stability analysis by considering four different cases corresponding to the possible values of α.

A. *Analysis of the* $\alpha = 0$ *case*

For the $\alpha = 0$ case, our dynamics (39) simplify to

$$\begin{aligned} \phi^{'} &= -\sin(\phi)\big(Pe^{\lambda} + 1\big), \\ \lambda^{'} &= P\left[e^{\lambda}\Big(1 - \cos(\phi)\Big) - 1\right] + \cos(\phi) + e^{\lambda}. \end{aligned} \tag{43}$$

Defining

$$H_0(\phi, \lambda) \triangleq -1 - \cos(\phi), \tag{44}$$

we have

$$H_0^{'} = -\sin^2(\phi)\big(Pe^{\lambda} + 1\big) = H_0(H_0 + 2)\big(Pe^{\lambda} + 1\big), \tag{45}$$

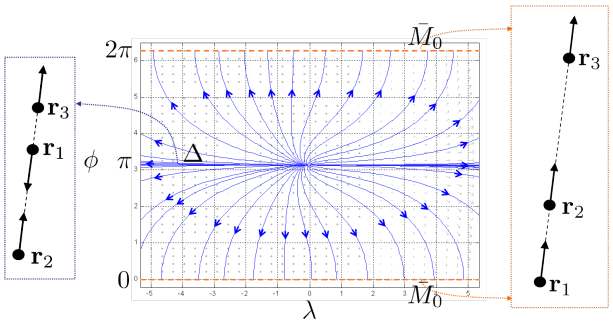

Fig. 4. Depiction of the $\{\phi, \lambda\}$ phase portrait for the $\alpha = 0$ case, which should be viewed as a (punctured) cylinder which has been cut along the set $\bar{M}_0$ and unwrapped. Also depicted are representative particle formations (from the full physical space) which correspond to each of the invariant submanifolds $\bar{M}_0$ and Δ.

from which it is apparent that the submanifolds defined respectively by $H_0 = 0$ and $H_0 = -2$ are both invariant under the dynamics (43). Noting that $H_0 = -2 \Longleftrightarrow \phi = 0$, we see that the latter invariant submanifold corresponds to our set of rectilinear equilibria $\bar{M}_0$ from (40). We define the other invariant submanifold as

$$\begin{aligned}\Delta &= \Big\{(\phi, \lambda) \in \bar{M}_{CB(0,0,\pi)} \;\Big|\; H_0 = 0\Big\} \\ &= \Big\{(\phi, \lambda) \in \bar{M}_{CB(0,0,\pi)} \;\Big|\; \phi = \pi\Big\}, \end{aligned} \tag{46}$$

noting that the one-dimensional reduced dynamics on Δ are characterized by $\lambda^{'} = 2e^{\lambda}\left(e^{\lambda} - 1\right)$, i.e. all trajectories on Δ move away from the point $\lambda = 0$. These two invariant manifolds (and representative particle formations on M_{state}) are depicted in the phase portrait[2] for the $\alpha = 0$ case, in figure 4. Since $\phi \in S^1$ and therefore $\phi = 0$ is identified with $\phi = 2\pi$, the phase portrait should be viewed as a punctured cylinder which has been cut along the set $\bar{M}_0$ and unwrapped.

The following proposition summarizes the stability analysis for the $\alpha = 0$ case, demonstrating that Δ is unstable and $\bar{M}_0$ is attractive on a large region of $\bar{M}_{CB(0,0,\pi)}$.

Proposition 5: Let $\bar{M}_{CB(0,0,\pi)}$, $\bar{M}_0$ and Δ be defined as in (33), (40) and (46) respectively. Any trajectory of (43) starting in the set

$$\bar{M}_{CB(0,0,\pi)} - \Delta \tag{47}$$

converges asymptotically to $\bar{M}_0$.

Proof: Let H_0 be defined as in (44), and define

$$\Omega_0^{\epsilon} = \Big\{(\phi, \lambda) \in \bar{M}_{CB(0,0,\pi)} \;\Big|\; H_0 \leq -\epsilon\Big\}, \tag{48}$$

where ϵ satisfies $0 < \epsilon \leq 2$. Note that Ω_0^{ϵ} is closed and positively invariant under the dynamics (43). From (45), it is clear that $H_0^{'} \leq 0$ on Ω_0^{ϵ} with $H_0^{'} = 0$ on Ω_0^{ϵ} if and only if $H_0 = -2$, which corresponds to the invariant set $\bar{M}_0$. Though Ω_0^{ϵ} is not bounded as a set, we claim that every trajectory of (43) which starts in Ω_0^{ϵ} is bounded. To prove this claim, we argue by contradiction. If such a trajectory were unbounded, then it must become unbounded in λ (since it cannot cross $\bar{M}_0$ or Δ). Since there are no equilibrium points contained in Ω_0^{ϵ} except for the set $\bar{M}_0$, and $H_0^{'} < 0$ on $\Omega_0^{\epsilon} - \bar{M}_0$, it must be that the trajectory asymptotically approaches the set $\bar{M}_0$ while becoming unbounded in the direction $\lambda = +\infty$ or $\lambda = -\infty$. However, by **Proposition 4** it holds that $\lim_{\phi \to 0} \frac{\partial \phi}{\partial \lambda} = -\infty$, and therefore $\bar{M}_0$ can not serve as an asymptote for the trajectory. Hence, the trajectory must be bounded, and therefore by Birkhoff's theorem the ω-limit set is nonempty, compact and invariant. Asymptotic convergence to $\bar{M}_0$ follows as in the steps in the proof of LaSalle's Invariance Principle [9]. Finally, since ϵ can be arbitrarily small, it follows that the region of convergence is given by $\bar{M}_{CB(0,0,\pi)} - \Delta$. □

B. Analysis of the $\alpha \in (-\pi/2, 0) \cup (0, \pi/2)$ case

For $\alpha \in (-\pi/2, 0) \cup (0, \pi/2)$, our dynamics are as stated in (39). The phase portrait (as displayed in figure 5 for $\alpha = \pi/3$) suggests that most trajectories converge asymptotically to the equilibrium set $\bar{M}_{\alpha}$, a result which we can prove analytically for trajectories which start in the shaded regions Ω_{α}^{+} and Ω_{α}^{-} (defined below).

Proposition 6: For any $\alpha \in (-\pi/2, 0) \cup (0, \pi/2)$, we define

$$\begin{aligned}\Omega_{\alpha} = \Big\{&(\phi, \lambda) \in \bar{M}_{CB(\alpha,\alpha,\pi+\alpha)} \;\Big| \\ &\cos(\phi) \geq \max\left[\cos(\alpha), |\sin(\alpha)|\right]\Big\}. \end{aligned} \tag{49}$$

Let $\bar{M}_{\alpha}$ be defined as in (40). Every trajectory of (43) starting in Ω_{α} converges asymptotically to $\bar{M}_{\alpha}$.

Proof: Due to space constraints, we provide only a sketch of the proof. As depicted in figure 5, if we define

$$\begin{aligned}\Omega_{\alpha}^{+} &= \Big\{(\phi, \lambda) \in \Omega_{\alpha} \;\Big|\; \sin(\phi) > 0\Big\}, \\ \Omega_{\alpha}^{-} &= \Big\{(\phi, \lambda) \in \Omega_{\alpha} \;\Big|\; \sin(\phi) < 0\Big\}, \end{aligned}$$

then the set Ω_{α} can be decomposed as $\Omega_{\alpha} = \Omega_{\alpha}^{+} \cup \bar{M}_{\alpha} \cup \Omega_{\alpha}^{-}$. By a rather lengthy analysis, one can demonstrate that $\phi^{'} < 0$ on Ω_{α}^{+} and $\phi^{'} > 0$ on Ω_{α}^{-}, and therefore the quantity $V = -\cos(\phi)$ satisfies $V^{'} \leq 0$ on Ω_{α} with $V^{'} = 0$ only on the set $\bar{M}_{\alpha} \subset \Omega_{\alpha}$. The proof then proceeds analogously to the proof of **Proposition 5**, using a similar argument to prove boundedness of trajectories and then applying the steps from the proof of LaSalle's Invariance Principle [9]. □

C. Analysis of the $\alpha = \pi/2$ case

Substitution of $\alpha = \pi/2$ into the dynamics (39) yields

$$\begin{aligned}\phi^{'} &= P\left[e^{\lambda}\Big(1 - \cos(\phi)\Big) - 1\right] + \cos(\phi) + e^{\lambda}, \\ \lambda^{'} &= \sin(\phi)\big(Pe^{\lambda} + 1\big). \end{aligned} \tag{50}$$

The phase portrait (displayed in figure 6) reveals some remarkable properties of the trajectories of these dynamics. Analogous to previous cases, the set $\bar{M}_{\pi/2}$ consists of a continuum of equilibria which correspond to rectilinear

[2]All phase portraits were created with the *pplane* tool for MATLAB, available at http://www.math.rice.edu/∼dfield/.

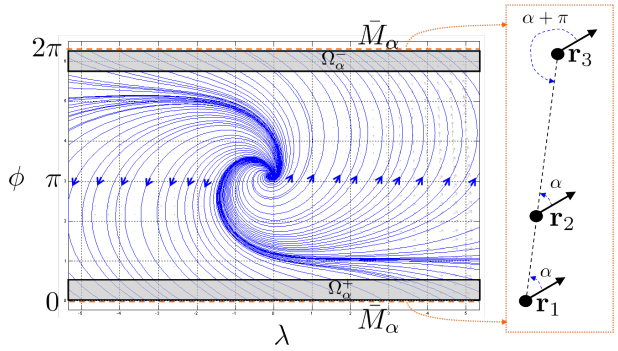

Fig. 5. Depiction of the $\{\phi, \lambda\}$ phase portrait for $\alpha = \pi/3$, representing the $\alpha \in \left(0, \frac{\pi}{2}\right)$ case. The dashed line is the set $\bar{M}_\alpha$, a continuum of equilibria for the dynamics (39) corresponding to rectilinear equilibria for the full dynamics (1). As stated in **Proposition 6**, trajectories which start in the shaded regions can be shown to converge asymptotically to $\bar{M}_\alpha$.

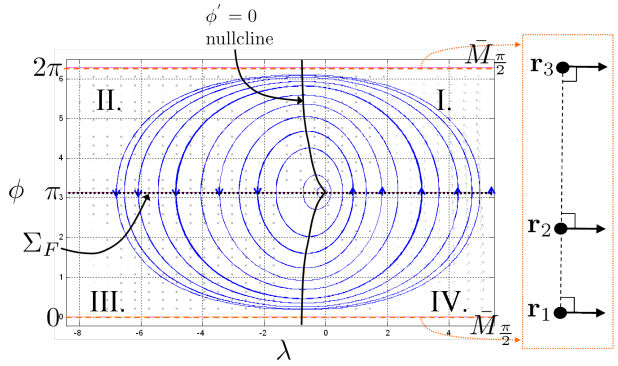

Fig. 6. Depiction of the $\{\phi, \lambda\}$ phase portrait for the $\alpha = \pi/2$ case. Analogous to previous cases, the set $\bar{M}_{\pi/2}$ consists of a continuum of rectilinear equilibria of the type shown. However, in this case the phase portrait indicates that all trajectories not starting on $\bar{M}_{\pi/2}$ are in fact periodic in the $\{\phi, \lambda\}$ space. Note that the solid black curve corresponds to the nullcline ($\phi' = 0$), and the dashed black line corresponds to the nullcline ($\lambda' = 0$), which is also the fixed-point set Σ_F for the reverser F defined in **Proposition 7**.

equilibria (of the type shown) in the full state space, but unlike the previous cases, there is no set on which trajectories converge asymptotically to $\bar{M}_{\pi/2}$. Rather, all trajectories that do not start on $\bar{M}_{\pi/2}$ exhibit periodic behavior in the $\{\phi, \lambda\}$ space, depicted in the phase portrait as counter-clockwise closed orbits. (Analogous clockwise orbits appear in the $\alpha = 3\pi/2$ case.) The corresponding particle trajectories in the plane display precession, as illustrated in figure 7. We proceed using the notion of reversible dynamics as in [10].

Definition 1 (Involution): A diffeomorphism $F : M \longrightarrow M$ from a manifold M to itself is said to be an *involution* if $F \neq id_M$, the identity diffeomorphism, and $F^2 = id_M$, i.e. $F(F(m)) = m, \forall m \in M$.

Definition 2 (F-reversibility): A vector field X defined over a manifold M is said to be *F-reversible* if there exists an involution F such that $F_*(X) = -X$, i.e. F maps orbits of X to orbits of X, reversing the time parametrization. Here $(F_*(X))(m) = (DF)_{F^{-1}(m)} X(F^{-1}(m))\ \forall m \in M$ is the push-forward of F. We call F the *reverser* of X.

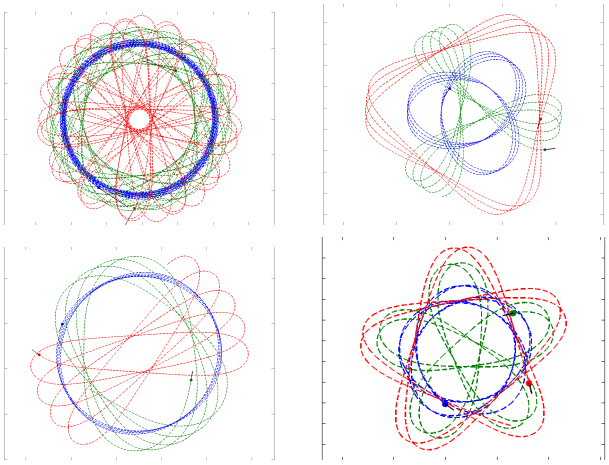

Fig. 7. These MATLAB plots illustrate 3-particle motions in the plane for different initial conditions arising in the $\alpha = \pi/2$ case. The associated phase space i.e. (ϕ, λ) trajectories are periodic, and result in the precessing behavior in physical space depicted here.

The following proposition establishes that the dynamics (50) are in fact F-reversible.

Proposition 7: The vector field defined by (50) is F-reversible, with reverser $F(\phi, \lambda) = (-\phi, \lambda)$.

Proof: Identifying the vector field from (50) as $X(\phi, \lambda)$, we have $X_1(\phi, \lambda) = \phi'$ and $X_2(\phi, \lambda) = \lambda'$. Observe from (38) that $P(-\phi, \lambda) = P(\phi, \lambda)$, and hence direct calculation from (50) establishes that $X_1(-\phi, \lambda) = X_1(\phi, \lambda)$ and $X_2(-\phi, \lambda) = -X_2(\phi, \lambda)$. Therefore,

$$\begin{aligned}(F_*(X))(\phi, \lambda) &= (DF)_{(-\phi,\lambda)} X(-\phi, \lambda) \\ &= \begin{bmatrix} -1 & 0 \\ 0 & 1 \end{bmatrix} \begin{bmatrix} X_1(\phi, \lambda) \\ -X_2(\phi, \lambda) \end{bmatrix} \\ &= -X(\phi, \lambda), \end{aligned} \tag{51}$$

which establishes the claim. □

Proposition 7 leads us to the following theorem of Birkhoff [11].

Theorem (G.D. Birkhoff): Let X be an F-reversible vector field on M and Σ_F the fixed-point set of the reverser F. If an orbit of X through a point of Σ_F intersects Σ_F in another point, then it is periodic.

For the fixed point set $\Sigma_F = \{(\phi, \lambda) : \phi = \pi\}$ of our reverser F (defined in **Proposition 7**), in order to employ Birkhoff's theorem to show all trajectories (not starting on $\bar{M}_{\pi/2}$) are periodic, we must show that all trajectories intersect Σ_F twice. (Note that here Σ_F is the nullcline ($\lambda' = 0$).) Numerical computation of the nullcline ($\phi' = 0$) with the MATLAB tool *pplane* clearly shows that the phase space is partitioned into four regions (see figure 6) with the characterization

region I: $\phi' > 0,\ \lambda' < 0$; region II: $\phi' < 0,\ \lambda' < 0$;
region III: $\phi' < 0,\ \lambda' > 0$; region IV: $\phi' > 0,\ \lambda' > 0$.

Then we proceed with the application of the Birkhoff theorem by (a) first showing that the trajectories starting on the portion of Σ_F which serves as the boundary between regions I and IV must reach the boundary between I and II, and (b) showing that a trajectory starting on the boundary between I and II must reach Σ_F in the portion that serves as the boundary between II and III. Then Birkhoff's theorem implies that in fact all orbits are periodic (except for equilibria on $\bar{M}_{\pi/2}$).

A purely analytical argument on the nature of the nullcline ($\phi^{'} = 0$) is being worked out.

Remark: If we define $\gamma \triangleq \ln(\rho_1)$, then for the $\alpha = \pi/2$ case we derive from (32)

$$\gamma^{'} = -\sin(\phi) P e^{\lambda}. \tag{52}$$

Having demonstrated that ϕ and λ are periodic with a common period (which we denote as T) and observing from (50) and (52) that $\gamma^{'} = -\lambda^{'} + \sin(\phi)$, we have

$$\begin{aligned}\gamma(\tau+T) - \gamma(\tau) &= \int_{\tau}^{\tau+T} \left[-\lambda^{'}(\sigma) + \sin(\phi(\sigma))\right] d\sigma \\ &= -\left[\lambda(\tau+T) - \lambda(\tau)\right] + \int_{\tau}^{\tau+T} \sin(\phi(\sigma)) d\sigma. \end{aligned} \tag{53}$$

By the periodicity of ϕ and λ and by the symmetry of trajectories about the set Σ_F (from **Proposition 7** and Birkhoff's theorem) it holds that (53) is zero and hence γ is also periodic with period T, i.e. the shape trajectories on $M_{CB(\frac{\pi}{2},\frac{\pi}{2},\frac{3\pi}{2})}$ are periodic. Finally, we note from (12) that the control inputs are also periodic.

D. Analysis of the $\alpha \in (\pi/2, 3\pi/2)$ case

For $\alpha \in (\pi/2, 3\pi/2)$, our dynamics are as stated in (39). The phase portrait, displayed in figure 8, reveals that the equilibria of $\bar{M}_\alpha$ are unstable in this case. Generic trajectories on $\bar{M}_{CB(\alpha,\alpha,\pi+\alpha)}$ tend to spiral in towards the excluded point $\phi = \pi, \lambda = 0$, which implies that $\rho_3/\rho_1 \longrightarrow 0$. Instability of the equilibria in $\bar{M}_\alpha$ follows since linearization of the dynamics (39) about an equilibrium point $(0, \lambda^0) \in \bar{M}_\alpha$ yields the Jacobian matrix

$$\left(e^{2\lambda_0} + e^{\lambda_0} + 1\right) \begin{bmatrix} -\cos(\alpha) & 0 \\ \sin(\alpha) & 0 \end{bmatrix}, \tag{54}$$

which has an eigenvalue at $-\left(e^{2\lambda_0} + e^{\lambda_0} + 1\right)\cos(\alpha) > 0$ (for $\alpha \in (\pi/2, 3\pi/2)$).

VI. Conclusion

In this work we have detailed a reduction of a $3n$-dimensional system to a $(2n-4)$ dimensional system (by way of symmetry, geometry, and constraint) in the context of multiple agents engaged in cyclic CB pursuit. For the case of $n = 3$, this reduction enabled an analysis of stability properties for a particular class of rectilinear equilibria by way of phase portrait analysis. For a certain choice of parameters, it was demonstrated that the 3-agent system exhibits infinitely many periodic orbits in the CB Pursuit Manifold $M_{CB(\frac{\pi}{2},\frac{\pi}{2},\frac{3\pi}{2})}$.

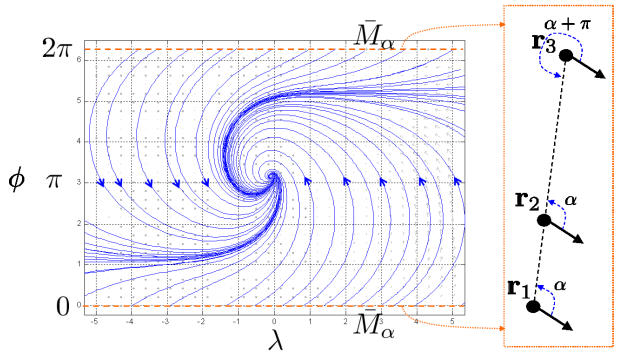

Fig. 8. Depiction of the $\{\phi, \lambda\}$ phase portrait for $\alpha = 2\pi/3$, representing the $\alpha \in (\pi/2, 3\pi/2)$ case. Here the equilibria of $\bar{M}_\alpha$ are unstable, and trajectories asymptotically approach $\phi = \pi, \lambda = 0$, i.e. $\rho_3/\rho_1 \longrightarrow 0$.

Ongoing work includes an analysis of stability properties for three-particle circling equilibria (as well as spiraling trajectories which preserve pure shape), and a characterization of three-particle cyclic CB pursuit trajectories in the full three-dimensional space.

References

[1] K.S. Galloway, E.W. Justh and P.S. Krishnaprasad, "Geometry of cyclic pursuit," *Proc. 48th IEEE Conf. Decision and Control*, 7485-7490, 2009. (See also extended version at http://www.isr.umd.edu/Labs/ISL/PURSUIT).

[2] K.S. Galloway, E.W. Justh and P.S. Krishnaprasad, "Cyclic pursuit in three dimensions," *Proc. 49th IEEE Conf. Decision and Control*, 7141-7146, 2010.

[3] M. Mischiati and P.S. Krishnaprasad, "Motion camouflage for coverage," *Proc. American Control Conference*, 6429-6435, 2010.

[4] J.A. Marshall, M.E. Broucke, and B.A. Francis, "Formations of vehicles in cyclic pursuit," *IEEE Trans. Automat. Control*, 49(11):1963-1974, 2004.

[5] M. Pavone and E. Frazzoli, "Decentralized policies for geometric pattern formation and path coverage," *J. Dyn. Sys., Meas., Control*, 129(5):633-643, 2007. doi:10.1115/1.2767658.

[6] T.J. Richardson, "Non-mutual captures in cyclic pursuit," *Annals of Mathematics and Artificial Intelligence*, 31:127-146, 2001.

[7] A. Chenciner and R. Montgomery, "A remarkable periodic solution of the three-body problem in the case of equal masses," *Annals of Mathematics*, 152:881-901, 2000.

[8] E. Wei, E.W. Justh and P.S. Krishnaprasad, "Pursuit and an evolutionary game," *Proc. R. Soc. A*, Vol. 465, 1539-1559, 2009. First published online Feb. 25, 2009, doi:10.1098/rspa.2008.0480.

[9] H.K. Khalil. *Nonlinear Systems (Third Edition)*. New Jersey: Prentice-Hall, 2002.

[10] M. Mischiati and P.S. Krishnaprasad, "The dynamics of mutual motion camouflage," *submitted for publication*, 2011.

[11] G.D. Birkhoff, "The restricted problem of three bodies," *Rendi. Circ. Mat. Palermo*, 39:265-334, 1915.